Memory Effects in Carbocation Rearrangements: Structural and Dynamic Study of the Norborn-2-en-7-ylmethyl-X Solvolysis Case

UNIVERSITÀ DEGLI STUDI DI TORINO

Memory Effects in Carbocation Rearrangements: Structural and Dynamic Study of the Norborn-2-en-7-ylmethyl-X solvolysis case.

Giovanni Ghigo,* Andrea Maranzana, Glauco Tonachini

Dipartimento di Chimica, Università di Torino, V. Giuria 7, I-10125 Torino, Italy

Abstract

The solvolysis of two diastereomers may give the same two products, but in different ratios, notwithstanding the two reaction pathways share an apparently identical intermediate carbocation. This was dubbed "*memory effect*", since the initial carbocation seems to "remember" its origin when undergoing further evolutions through multi-step rearrangements. This puzzling result is studied theoretically for the case of the solvolysis of norborn-2-en-7-ylmethyl-X systems, by defining the reaction potential energy surface, (PES) then carrying out a dynamical study. The PES shows that upon X^- loss multi-phase rearrangements concertedly yield the two stablest carbocations **G** and **L**. These carbocations are connected by a transition structure. The carbocation intermediates proposed in the literature do not correspond to any stationary point. The preference for the rearrangement to **G** or **L** (the *memory effect*) is determined by structural and stereoelectronic effects: the competitive interaction between an empty *p* orbital with a σ orbital or with a *p*/π orbital is guided by geometrical aspects present in the starting carbocations. The dynamic study shows that: (1) **G** and **L** do not interconvert; (2) the evolving system can switch from one pathway to the other to different extents, thus determining a more or less pronounced memory loss (the *leakage*).

KEYWORDS: Memory effect, Rearrangement, Carbocation, Stereoelectronic effect, DFT, Dynamic

* Correspong author giovanni.ghigo@unito.it

Introduction

The *memory effect*[1] is a stereochemical control on a reaction center operated by a different center localized on the same molecule. The most known case is the neighboring group effect which leads to maintain the configuration in some solvolyses (Scheme 1 shows two examples[2]).

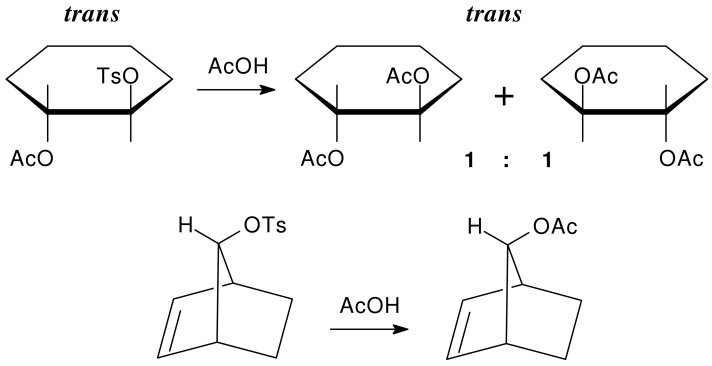

Scheme 1. *Memory effect* due to neighboring group effect.

In some cases such a control can be exercised by a more remote center. In particular, the *memory effect* has been invoked in the multiple rearrangement of carbocations when the two stereoisomers of the precursor rearrange to different products despite the apparent existence of some common intermediate along the reaction pathway. This case is illustrated by Scheme 2 which shows the solvolysis with rearrangement of **R-X** which takes place through carbocation intermediates $\mathbf{R}^+$ and $\mathbf{M}^+$. Here we can see that the solvolysis of the stereoisomer **R'-X** mainly yields product **P'** while that of the stereoisomer **R"-X** mainly yields product **P"**. The presence of a memory effect is testified by the fact that intermediates $\mathbf{R"}^+$ and $\mathbf{R'}^+$ are expected to easily interconvert because linked by a simple conformational relation (in contrast to being just the same structure, which would leave the effect unexplained). The picture is completed

by the observation that the solvolysis of **M'-X** yields exclusively product **P'** while the solvolysis of **M"-X** yields exclusively product **P"**. Intermediates **M'**$^{+}$ and **M"**$^{+}$ are structural isomers (not just stereoisomers) and they do not interconvert. Their formation from **M'-X** and **M"-X** involves a rearrangement often with some neighboring group effect.

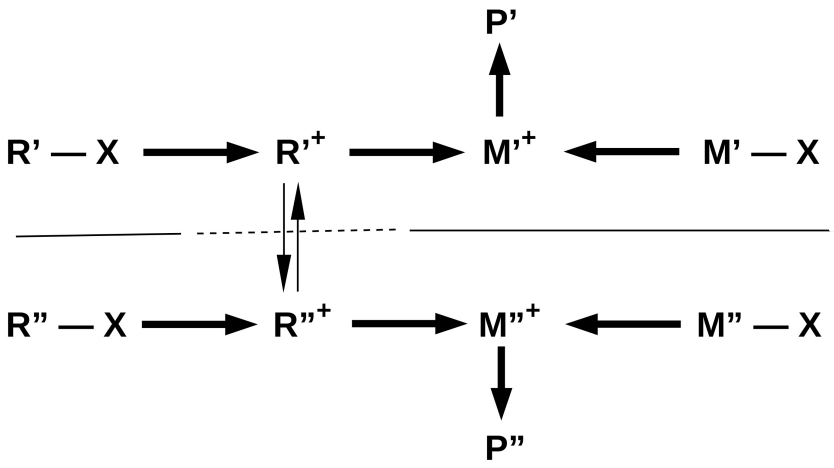

Scheme 2. The *memory effect* in the multiple carbocation rearrangement.

This kind of stereochemical control was first observed as early as in 1961 by Marc Silver[3] and one year later by Jerome Berson and coworkers[4] who dubbed it *memory effect*.[1] Other studies by Berson and coworkers followed in the 60s[5] and by Clair Collins in the first 70s.[6] Despite the the great amount of experimental work, the causes of the *memory effect* are not fully understood. Therefore, we have undertaken the study of this stereochemical control by theoretical methods. We have chosen, among several cases, the norborn-2-en-7-ylmethyl cation derived from acetolysis of different **X**-substituted norborn-2-en-7-ylmethyl systems which is the most famous case.[7] Starting from its *syn* (**II**$_s$) and *anti* (**I**$_a$) diastereomers (Scheme 3), beside small amounts of the products of the simple solvolysis (**III**$_s$ and **III**$_a$) they also observed

the formation of different amounts of the two distinct products belonging to the so called Goering[8] series (**VIII** from carbocation **G**) and Le Bel[9] series (**IX** from carbocation **L**). In his paper, Berson suggested that after the ionic detachment of the leaving groups the two norborn-2-en-7-ylmethyl carbocations $\mathbf{II}_s$ and $\mathbf{II}_a$, before the capture of the solvent, can rearrange to cations $\mathbf{IV}_s$ and $\mathbf{IV}_a$. These two carbocations could yield the product of solvent capture **VI'** and **VI"** (found, indeed, in very small amounts) or give rise to a second rearrangement leading, respectively, to the final products from cation **G** (from $\mathbf{I}_s$) and from cation **L** (from $\mathbf{I}_a$). The observation that the solvolysis of the *syn* isomer $\mathbf{I}_s$ mainly leads to product **G**, while that of the isomer *anti* $\mathbf{I}_a$ mainly leads to product **L** through cations $\mathbf{IV}_s$ and $\mathbf{IV}_a$, which are just two conformers of the same carbocation, suggests the existence of some sort of "*memory effect*" that make the two cations "to remember" from which cation they come. Indeed, in the solvolysis of $\mathbf{I}_a$ small amount of product **L** were also found and, by converse, in the solvolysis of $\mathbf{I}_a$ small amount of product **G** were also found. This suggested the occurrence of some equilibration between the two cations $\mathbf{IV}_s$ and $\mathbf{IV}_a$ through a transition structure **V** or, possibly, the existence of an intermediate structure **V** which connects cations $\mathbf{IV}_s$ and $\mathbf{IV}_a$. This equilibration determinates a partial loss of the *memory effect*, a phenomenon known as *leakage*.

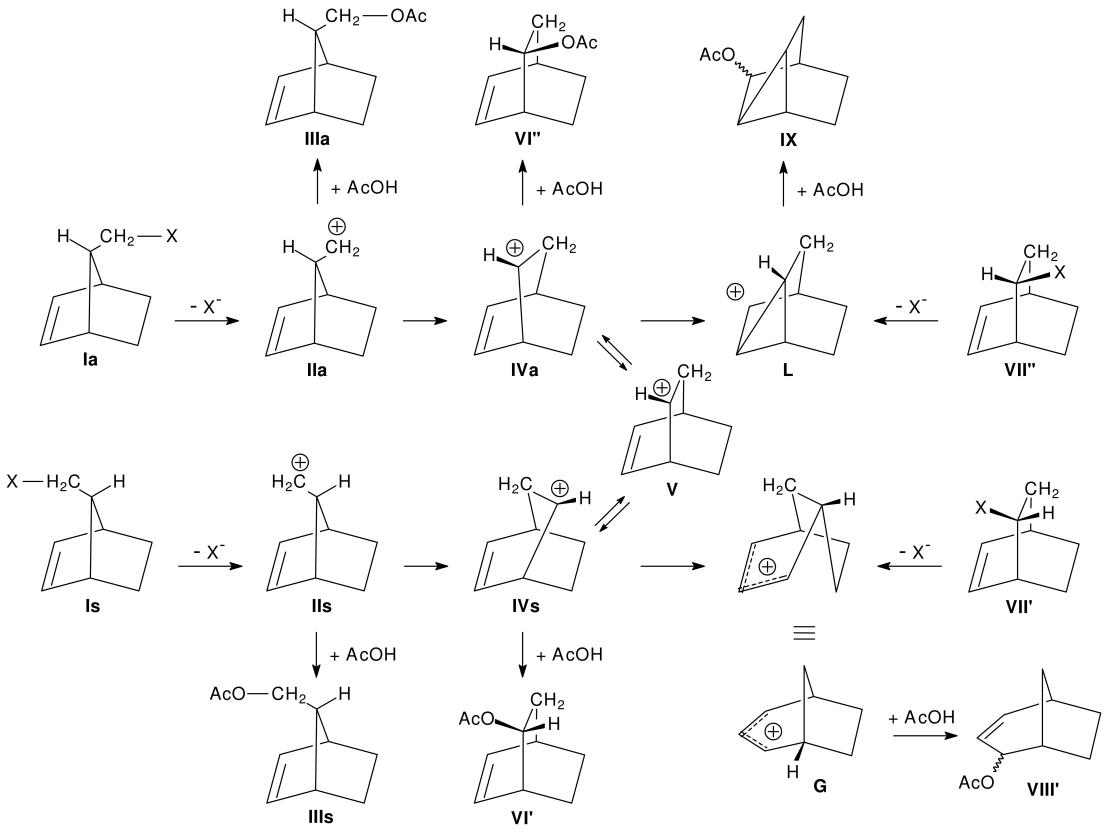

Scheme 3. The *memory effect* as proposed in the literature.

Despite the elegance of scheme 3, a full comprehension of this phenomena was not achieved: the experimental findings (isotope labelling and a substantial lack of ion-couples and solvent effects) only demonstrated that the "*memory must be preserved in processes passing through carbonium ions, not bimolecular nucleophilic reactions*." A role for a "asymmetric ionic solvation" was also excluded by Berson.[5d] Collins[6c] proposed this role again, but his experiments were performed on completely different systems. Another fact complicates the picture: the solvolysis of the two tosylates of 2-bicyclo[2.2.2]oct-5-enyl (**VII'** and **VII"**) only yields the products of the rearrangement: the acetate **VIII** of cation **G** from **VII'** and the acetate **IX** of cation **L** from **VII"**.[5a] This result confirms that the equilibration, if any, it is not between cations **G** and **L**. However, considering that the heterolysis of the two

tosylates must form cations **IV**$_s$ and **IV**$_a$ it is hard to explain why there is not a partial loss of the *memory effect* that would yield again to the formation of the acetates of cation **G** from **VII"** and of cation **L** from **VII'**. In the experiments[5a] several leaving group were used and in all cases the *memory effect* with some *leakage* was observed. Table 1 collects the different cases. We stress that, without *leakage*, the solvolysis of the *syn* isomer should only yield the acetates of **G** while that of the *anti* isomer, the acetates of **L**. We can observe that the solvolysis of the *syn* isomer presents quite an extended *leakage* while the solvolysis of the *anti* isomer presents a quite extended *memory* of the starting molecule.

Table 1. Yield ratios and excesses[a,b] of acetates of cations **G** and **L** in the solvolysis of the norborn-2-en-7-ylmethyl derivatives **I**$_s$ and **I**$_a$.

Leaving group	*syn* (**I**$_s$)		*anti* (**I**$_a$)	
X	G/L	excess G[a]	L/G	excess L[b]
N_2 (from NH_2)	3 - 5	45 - 65	30 - 70	94 - 97
ONs	3 - 5	47 - 64	3.5 - 4.5	56 - 64
Br	2 - 4	33 - 64	42 - 45	82 - 96

[a] Per cent excess G = 100(G-L)/(G+L); [b] Per cent excess L = 100(L-G)/(L+G).

The nature of the leaving group changes the relative yields but the presence of the *memory effect* and the different extent of the *leakage* for the *syn* and *anti* isomers is unchanged. In the main part of our study the leaving groups and the solvent molecules are not present. This will not allow us to observe the effect of the leaving groups on the yields and the alternative pathways as deprotonation (which are, however, experimentally[5] found negligible). However, the experiments[5] proved that the rearrangements only involve carbonium

ions, that the ion-couples are excludes and, more important, that no products of the counterion recapture were isolated.

Our goal is to unravel the most important factors that lead to the *memory effect* and the *leakage* phenomenon. Therefore, our computational study is mainly focused on the free carbocations starting from the cations **II**$_s$ and **II**$_a$ after a preliminary analysis of their generation.

Results and discussion

The formation of cations **II**$_s$ and **II**$_a$ is a consequence of the heterolysis of the **C—X** bonds in **I**$_s$ and **I**$_a$, respectively, induced by the ionizing solvent. In the former, the heterolysis can also generate the non-classical carbocation **II**$_s$ (Scheme 4). The study of the heterolysis in the diazonium derivatives[10] (**X** = N_2^+, Table 2 and Figure 1) shows that the formation of **II**$_s^{NC}$ is negligible with respect to the formation of **II**$_s$ (from all three methods, yield is estimated < 0.5% at room temperature).

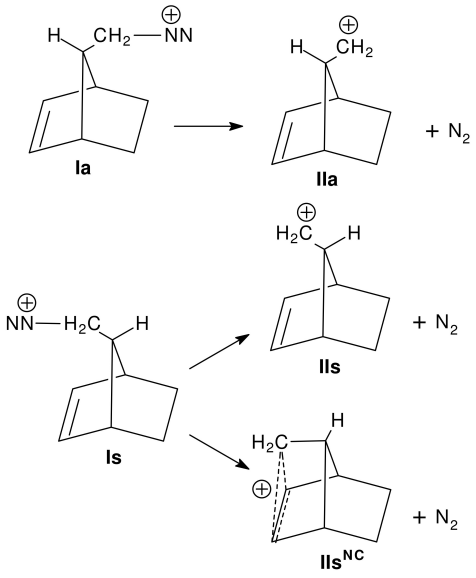

Scheme 4. The generation of carbocations from the solvolysis of norborn-2-en-7-ylmethyldiazonium.

Table 2. Relative energies ($\Delta E+\Delta ZPE$ in kcal mol^{-1}) in the solvolysis of norborn-2-en-7-ylmethyldiazonium.

Structure	ΔE^a	ΔE^b	ΔE^c
I$_s$—NN$^+$	0.0	0.0	0.0
TS to **II$_s$** + **N$_2$**	5.0	8.2	8.0
TS to **II$_s^{NC}$** + **N$_2$**	9.3	11.8	11.3
I$_a$—NN$^+$	2.2	2.1	2.0
TS to **II$_a$** + **N$_2$**	7.3	10.5	10.2

[a] B3LYP energies; [b] mPW1PW91 energies; [c] BB1K energies.

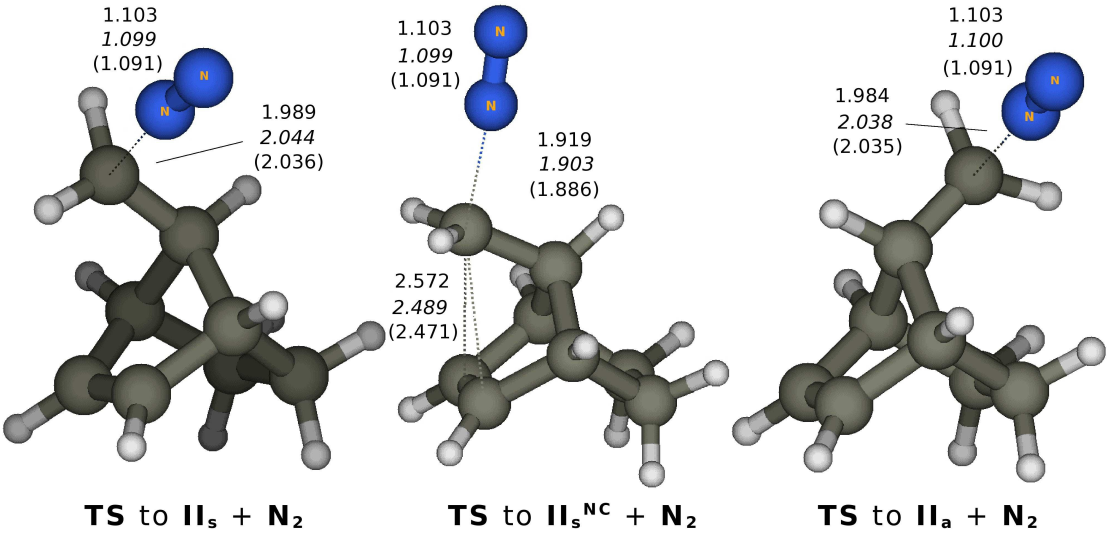

Figure 1. Transition structures of the solvolysis of norborn-2-en-7-ylmethyldiazonium. Plain figures: B3LYP; italics: mPW1PW91; in parenthesys: BB1K.

Once the transition structures (TS) are overcome we assume, on the basis of the experimental evidences, that **X** moves apart and leaves the reacting system. Therefore, we can proceed with our main intent which is to confirm the existence, on the potential energy surface (PES), of the carbocation intermediates shown in Scheme 3. The PES is illustrated by the More O'Ferrall-Jencks plot (Figure 2) where **R$_{CC}$** is the distance between **C^4** and **C^8**, **r$_1$** is the distance between **C^7** and **C^2**, and **r$_2$** is the distance between **C^7** and **C^6** (although important, distance

C^4—C^7 is not shown in the bidimensional plot). On the right side of the plot (at long R_{CC}, r_2–r_1 close to zero, and short C^4—C^7) we find cations II_s and II_a while in the left side (short R_{CC} and long C^4—C^7) we find cations **L** (at r_2–$r_1 \approx 0.9$) and **G** (at r_2–$r_1 \approx -0.9$).

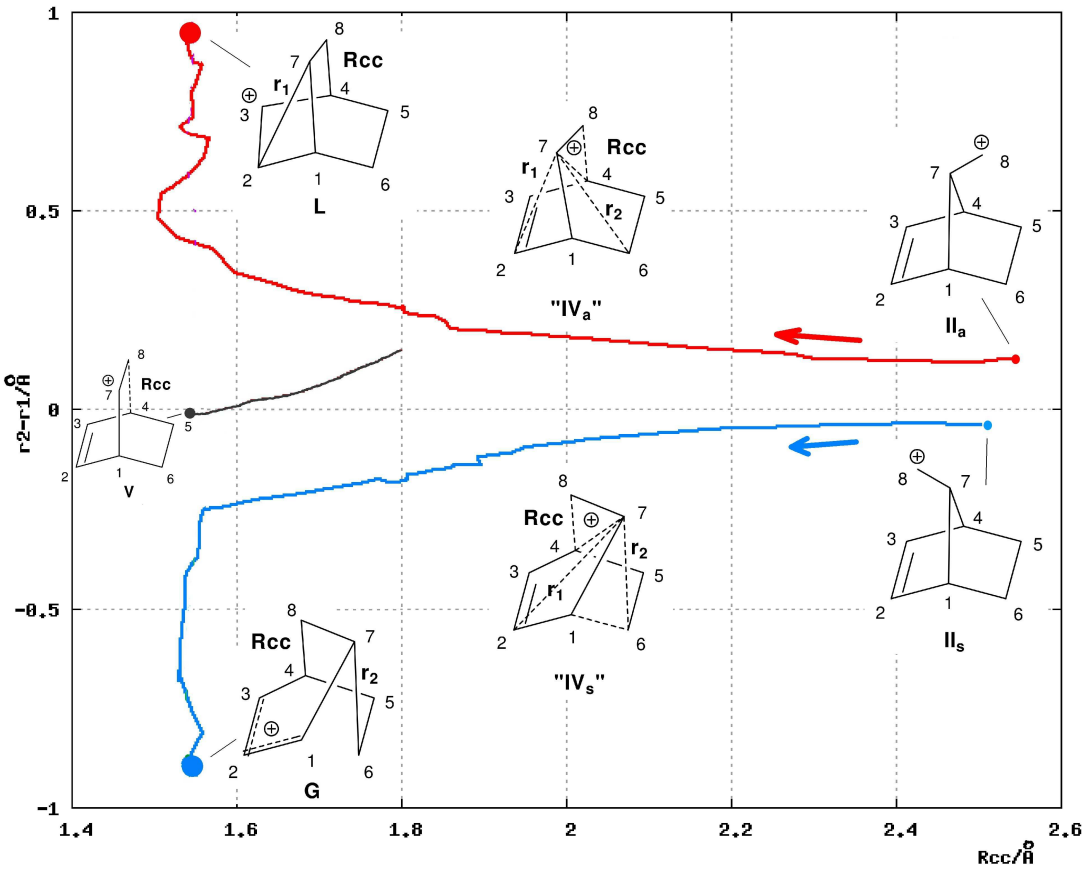

Figure 2. More O'Ferrall-Jencks diagram of the B3LYP IRCs for the rearrangement of cations II_s (blue line) and II_a (red line) and the ridge from TS **V** (grey line). The positions of cations **V**, **G**, and **L** are indicated by dots. R_{CC} is the distance C^4—C^7; r_1 is the distance C^7—C^2; r_2 is the distance C^7—C^6. Values are in Å.

The cation **G** (blue big dot in Figure 2, left, and Figure 3) is the most stable structure, since it contains a 1,3-disubstituted allyl system. Therefore, it is used as energy reference in Table 3. **G** and **L** (a secondary carbocation stabilized by a fused three-carbon ring, ΔE = 2-7 kcal mol^{-1}, red big dot in Figure 2, left, and Figure 3) are found to be real intermediates. Cation II_s^{NC} is the non-classical carbocation originated by the alternative solvolysis of I_s. Because its formation is

negligible (see Table 2) further evolutions are not analyzed.

Table 3. Relative energies ($\Delta E+\Delta ZPE$ in kcal mol^{-1}) in the rearrangement of carbocations **II**$_s$ and **II**$_a$.

Structure	ΔE^a	ΔE^b	ΔE^c
II$_s$	44.2	44.2	42.9
II$_s^{NC}$	31.5	24.8	20.0
II$_a$	47.3	47.3	46.1
V	17.6	16.8	16.8
L	7.1	3.6	1.7
G	0.0	0.0	0.0

[a] B3LYP energies; [b] mPW1PW91 energies; [c] BB1K energies.

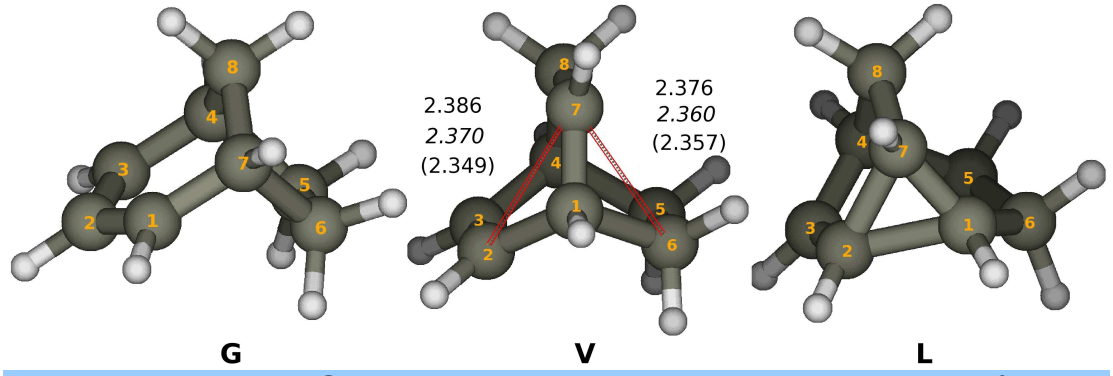

Figure 3. Cations **G** and **L** and transition structure **V**. Plain figures: B3LYP; italics: mPW1PW91; in parenthesys: BB1K.

By contrast, cations **IV**$_s$ and **IV**$_a$ do not exist as stationary points on the PES. Moreover, the structures **II**$_s$ and **II**$_a$ (primary carbocation structures, Figure 2, right) and **V** (a secondary carbocation structures) are found, indeed, to be transition structures and not stable cations. In particular, TS **V** (17 kcal mol^{-1}, grey dot in Figure 2, left, and Figure 3) directly connects cations **G** and **L**. The grey line in Figure 2 is the

ridge that originates from **V** and that "separates" the **G** region from the **L** region. From a stereochemical point of view, we can see (Figure 4) that the empty *p* orbital on $\mathbf{C^7}$ gives two competing stabilizing orbital interactions: one with the σ orbital of the $\mathbf{C^1}$—$\mathbf{C^6}$ bond (leading to cation **G**), the other with the *p*/π orbital on $\mathbf{C^2}$ (leading to cation **L**). In this almost symmetrical structure ($\mathbf{r_1}$=2.386 Å, $\mathbf{r_2}$=2.376 Å) there is a balance between the two interactions that "pull" $\mathbf{C^7}$, respectively, towards $\mathbf{C^6}$ or $\mathbf{C^2}$ in the transition structure **V**.

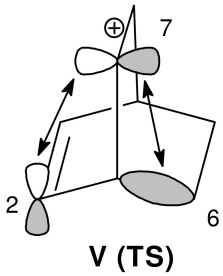

Figure 4. Orbital interactions in the carbocationic structure **V**.

In $\mathbf{II_s}$ (44 kcal mol^{-1} with respect to **G**) and $\mathbf{II_a}$ (46-47 kcal mol^{-1}) the vibrational mode with imaginary frequency corresponds to the stretching $\mathbf{C^4}$—$\mathbf{C^7}$ (or $\mathbf{C^1}$—$\mathbf{C^7}$) bond and the oscillation of $\mathbf{C^8}$ towards $\mathbf{C^4}$ (or towards $\mathbf{C^1}$).

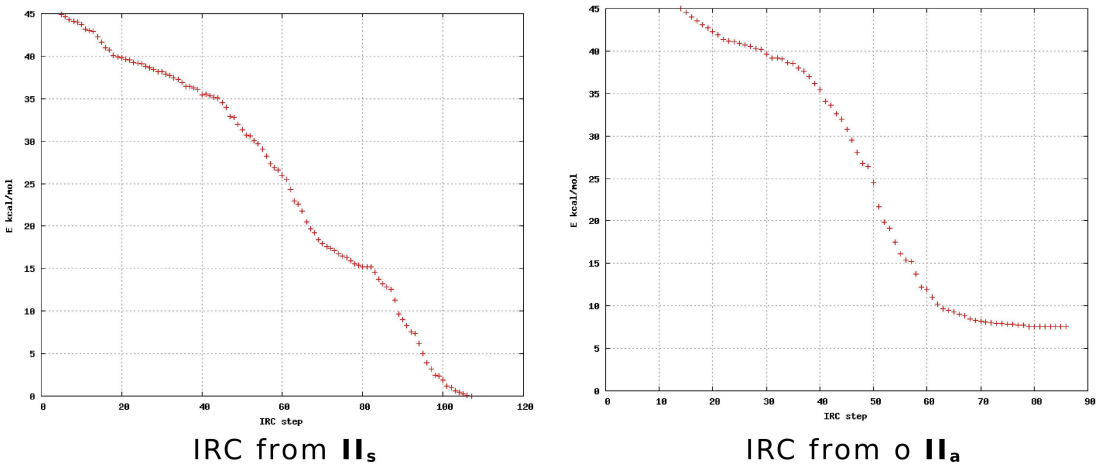

Figure 5. Energy profiles of along the B3LYP IRCs for the rearrangement of cations $\mathbf{II_s}$ (left) and $\mathbf{II_a}$ (right).

The IRCs (Figure 5) pathways (the blue and red lines starting from the right side in Figure 2) show that this atom displacements correspond to the "first rearrangement" of cations **II**$_s$ and **II**$_a$ that should yield the more stable secondary carbocations **IV**$_s$ and **IV**$_a$. These structures, however, do not correspond to stationary points on the PES (they are neither minima nor transition structures), in such a way that the chemical process does not stop in a single step and while **C**^{8}—**C**^{4} bond completes its formation ($\mathbf{R}_{CC}$ gets below 1.6 Å), carbon **C**^{7} bends towards **C**^{6} (if coming from **II**$_s$) or towards **C**^{2} (if coming from **II**$_a$) giving rise to the "second rearrangement". A "slight-shoulder",[11a] which appears in the energy profile of the IRC from **II**$_s$, around the 80th point, hints to a structure as carbocation **IV**$_s$. Yet, this structure cannot be considered as a proper intermediate, since it does not correspond to an energy minimum. By contrast, the energy profile for the IRC from **II** (Figure 5, right) does not suggest the existence of any carbocation intermediate. So, each reaction path follows a curve (left side in Figure 2) which finally yields either cations **G** or **L** describing a "*two-stages*" asynchronous concerted processes.[11] The More O'Ferrall-Jencks plot clearly shows the nature of the *memory effect*: in both rearrangements cations **IV**$_s$ and **IV**$_a$ are not present on the PES as stationary points, in such way that the structure of the starting carbocations determines the final products. In fact, in cation **II**$_s$ the distance between **C**^{7} and **C**^{6} ($\mathbf{r}_2$) is already shorter than the distance between **C**^{7} and **C**^{2} ($\mathbf{r}_1$). Therefore, when the rearrangement starts **C**^{7} is attracted by the **C**^{6} center ($\mathbf{r}_2$–$\mathbf{r}_1$ become more negative) because the orbital interaction between incipient empty *p* orbital on **C**^{7} with the σ orbital of the **C**^{1}—**C**^{6} bond prevails. Consequently, the two rearrangements take place concertedly (though asynchronously) to

finally yield the cation **G**. The same structural guidance occurs for cation $\mathbf{II_a}$, where the shorter distance between $\mathbf{C^7}$ and $\mathbf{C^2}$ ($\mathbf{r_1}$, $\mathbf{r_2}-\mathbf{r_1}$ positive) dictates a concerted rearrangement to the cation **L**. In this case it is the interaction between the incipient empty *p* orbital on $\mathbf{C^7}$ with the p/π orbital on $\mathbf{C^2}$ to prevail. In both cases the rearrangements are quite exothermic (by more than 40 kcal mol^{-1}). Therefore, the PES can be described as two valleys originated from $\mathbf{II_s}$ and $\mathbf{II_a}$ and separated by a ridge originated from **V**. The topology of this case seems to differs from that studied found by other authors where the the key point is a valley bifurcation leading to two minima on the PES.[12]

The structural reasons explain the *memory effect* but the occurrence of the *leakage* is not covered yet. At first sight, the *leakage* could be the explained by the interconversion of cations **G** and **L** through **V**. However, as reported above, the solvolysis of **VII'** and **VII"** excludes this possibility, and the *leakage* must take place in a different way. As we can see on the right side of Figure 2, in the initial phase of the rearrangements, $\mathbf{r_2}-\mathbf{r_1}$ (and therefore $\mathbf{r_1}$ and $\mathbf{r_2}$) only changes by a small amount until $\mathbf{R_{CC}}$ gets below 1.8-9 Å. Therefore, it is possible that dynamics effects[12,13] could allow the two pathways to cross one each other. This is just what we verified by using a Born-Oppenheimer Molecular Dynamics model (see Method section) calculations. The resulting trajectories are shown in two More O'Ferrall-Jencks diagrams: Figure 6 for the rearrangement taking origin from TS $\mathbf{II_s}$ and Figure 7 for the rearrangement from TS $\mathbf{II_a}$.

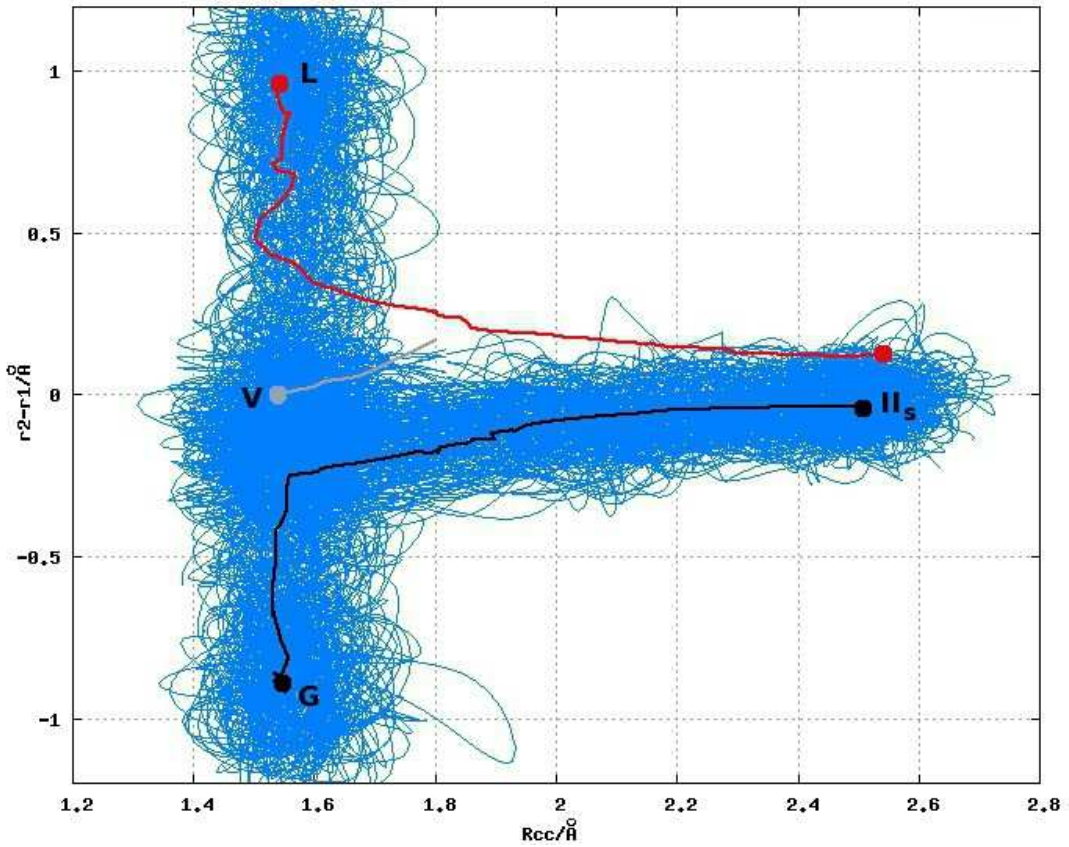

Figure 6. Trajectories (More O'Ferrall-Jencks diagram) relevant to rearrangement of cation $\mathbf{II_s}$. For $\mathbf{R_{CC}}$, $\mathbf{r_1}$, and $\mathbf{r_2}$ see caption to Figure 2.

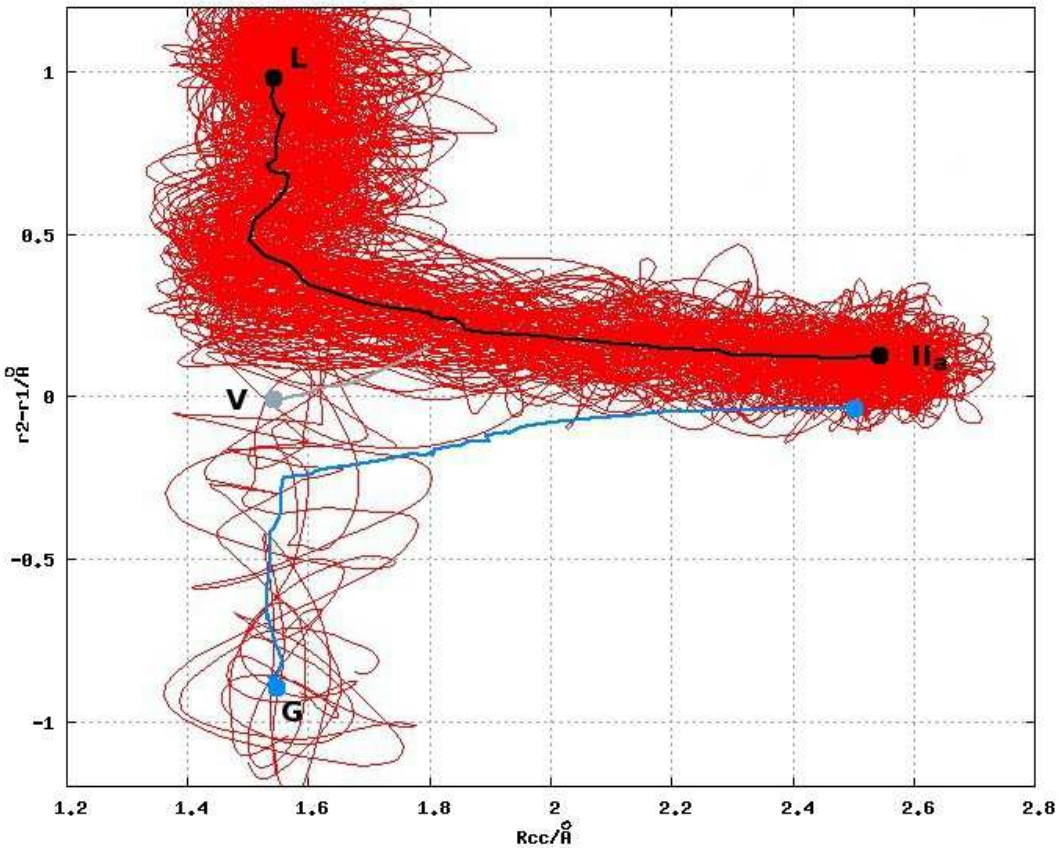

Figure 7. Trajectories (More O'Ferrall-Jencks diagram) relevant to rearrangement of cation $\mathbf{II_a}$. For $\mathbf{R_{CC}}$, $\mathbf{r_1}$, and $\mathbf{r_2}$ see caption to Figure 2.

In Figure 6 we can see that about half of the trajectories from **II**$_s$ leads to cation **L** instead of cation **G**. The **G**/**L** ratio is 1.0 and the excess of **G** is only 2%. By contrast, in Figure 7 we can see a great majority of trajectories from **II**$_a$ goes to the expected cation **L** while only a few go to cation **G**. This corresponds to a **L**/**G** ratio of 27 and an excess of **L** of 96%. These values are in qualitative agreement with the experimental findings (compare Table 1): in the rearrangement of that follows TS **II**$_a$ the *memory effect* is more efficient (less *leakage*) than in the rearrangement that follows TS **II**$_s$. The oscillation of the trajectories could also allow solvent capture yielding the minor products and **III**$_s$, **III**$_a$, **VI'**, and **VI"**. Comparing Figures 6 and 7 we can observe that when the **C**^{8}—**C**^{4} bond formation is almost complete ($\mathbf{R}_{CC}$ below 1.7 Å), the trajectories from **II**$_s$ oscillates around **V** and its ridge (the grey line) while the trajectories from TS **II**$_a$ oscillates definitely in the **L** region (above the ridge from **V**) determining the greater *leakage* in the rearrangement of **II**$_s$. This behavior can also be observed in Figures 8 and 9 that report the values of $\mathbf{R}_{CC}$ and $\mathbf{r}_2$–$\mathbf{r}_1$ as function of the time. In the rearrangement that follows TS **II**$_s$ we can see (Figure 8, blue lines) that the **C**^{8}—**C**^{4} bond forms ($\mathbf{R}_{CC}$ oscillates around 1.5 Å) within a time ranging between 90 to 150 femtoseconds (fs). The evolution of $\mathbf{r}_2$-$\mathbf{r}_1$ shows on the other hand that **C**^{7} starts to bend towards **C**^{2} or **C**^{6} only after 140 fs (Figure 8, green lines). By contrast, in the rearrangement that follows TS **II**$_a$ we can see (Figure 9, red lines) that while the **C**^{8}—**C**^{4} bond also forms within 80-140 fs, **C**^{7} starts to bend towards **C**^{2} or **C**^{6} (Figure 9, green lines) already after 80 fs. Moreover, we can observe (green lines in Figures 8 and 9) that when **G** or **L** are formed, *i.e.* $|\mathbf{r}_2\text{-}\mathbf{r}_1| > 0.5$ Å, the trajectories do not cross any longer the line $\mathbf{r}_2$-$\mathbf{r}_1 = 0$ Å, *i.e.* **G** and **L** do not interconvert through **V**.

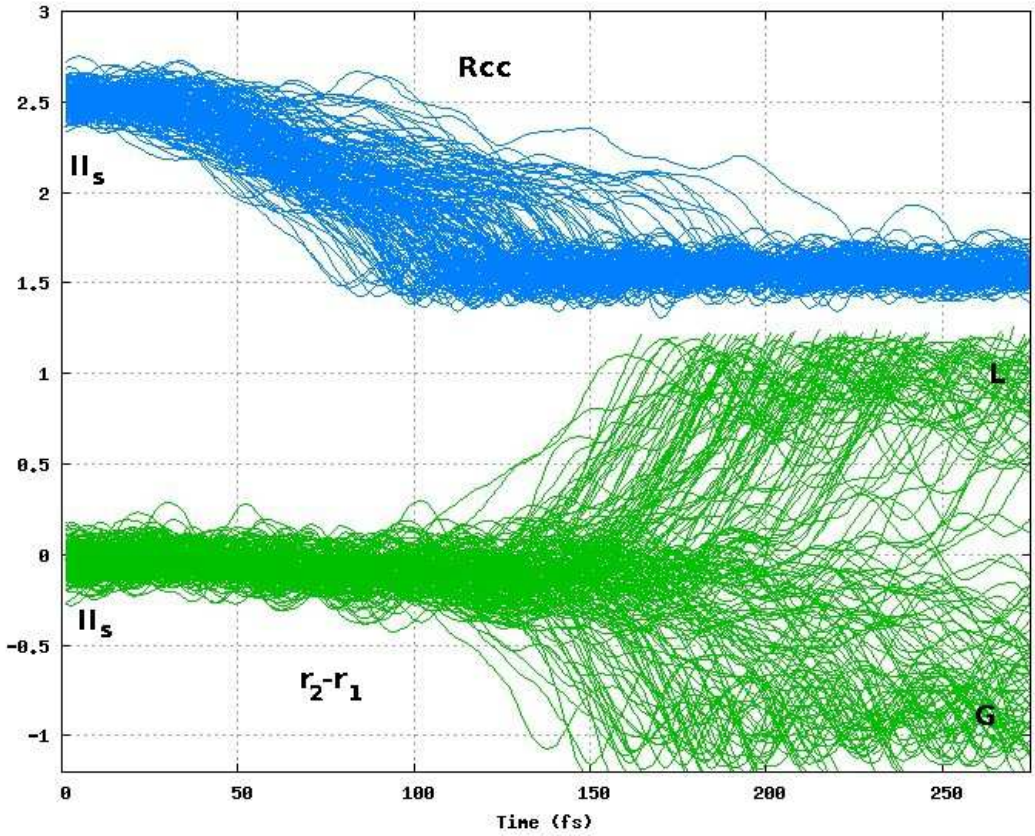

Figure 8. Trajectories as a function of time (fs) relevant to rearrangement of cation Π_s. Blue lines $\mathbf{R}_{CC}$, green lines $\mathbf{r}_2$-$\mathbf{r}_1$.

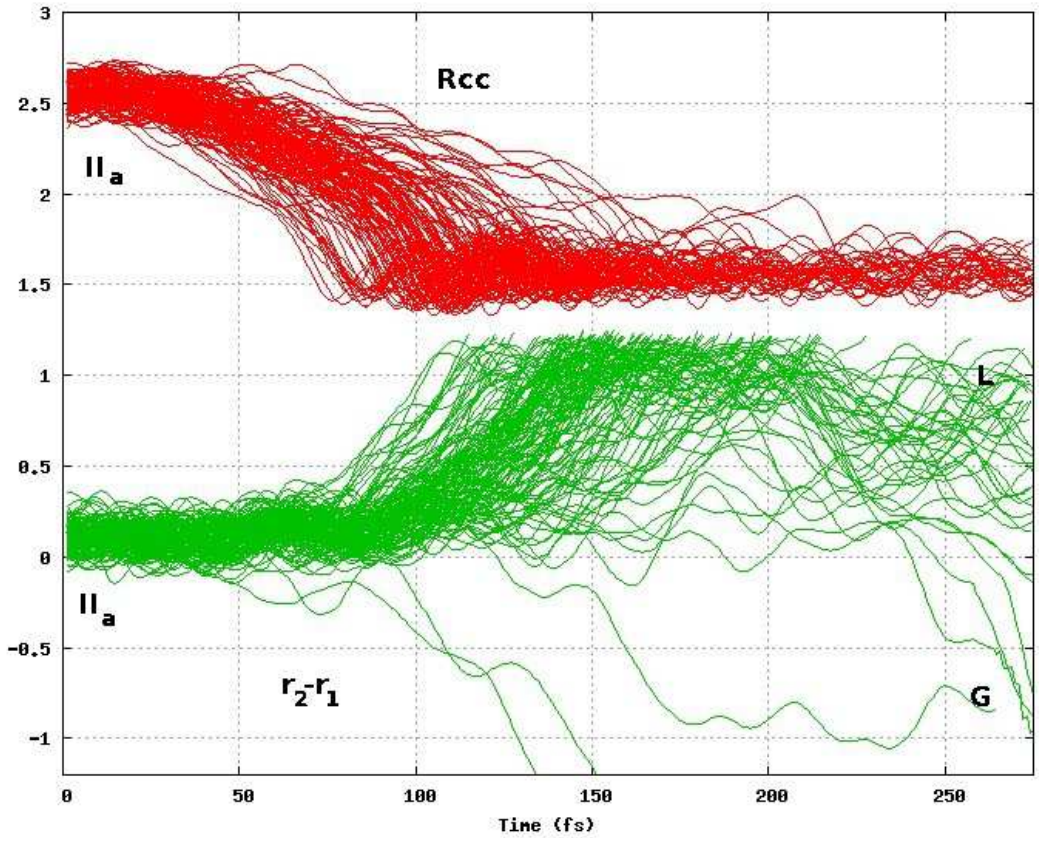

Figure 9. Trajectories as a function of time (fs) relevant to rearrangement of cation Π_a. Red lines $\mathbf{R}_{CC}$, green lines $\mathbf{r}_2$-$\mathbf{r}_1$.

In both cases the "*first rearrangement*" (formation of **C**^{8}—**C**^{4} bond) is complete within 150 fs, quite similar to other cases,[13,14] while the "*second rearrangement*" (formation of **G** or **L**) requires a longer time. A possible explanation (compare Figure 4) for the different extent of *leakage* is that being the *p*/π orbital more diffuse than the σ orbital, the interaction of incipient empty *p* orbital on **C**^{7} (particularly when the **C**^{4}—**C**^{8} bond is already formed) with the former is more effective than the interaction with the latter. Therefore, during the oscillation of the trajectories beyond TS **II**$_{s}$ along and in some proximity of the corresponding IRC pathway (black line in Figure 2) the interaction with the *p*/π orbital can prevail, in some cases, on the interaction with the σ orbital leading the rearrangement towards cation **L** (instead of **G**) so giving rise to the *leakage*. In the rearrangement beyond TS **II**$_{a}$ the interaction of the empty *p* orbital with the *p*/π orbital (leading to **L**) is further favored by structural reasons (**C**^{7} closer to **C**^{2}) so less *leakage* is observed.

Conclusions

The *memory effect* in the rearrangement of the two carbocations generated in the solvolysis of the *syn* and *anti* norborn-2-en-7-ylmethyl-**X** systems (**I**$_{s}$ and **I**$_{a}$) has been explained here as being determined by the different interactions that build up along the rearrangement pathways cationic systems. The parameter $\mathbf{r}_2-\mathbf{r}_1$ determines which is the dominant stabilizing orbital interaction (see Figure 4) of the incipient empty *p* orbital on **C**^{7}: that with the *p*/π orbital on **C**^{2} (which leads to cation **L**) or, alternatively, the one with the σ orbital of the **C**^{1}—**C**^{6} bond (which leads instead to cation **G**).

The study of the PES has shown that the carbocations **IV**$_s$ and **IV**$_a$ (Scheme 3), proposed in the literature, do not exist as stationary point on the PES, and that structure **V** is a TS connecting cations **G** and **L**. PES and dynamic studies (and experiments[5a] with **VII'** and **VII"**) then shows that **V** has no role despite its low energy with respect to cations **G** (17 kcal mol^{-1}) or **L** (10-15 kcal mol^{-1}). These energy barriers should lead products from cation **G** to prevail but this would disagree with the experimental findings. Moreover, when dynamics effects are introduced, the oscillation of the rearrangement trajectories can overcome the initial structural guidance, responsible of the *memory effect*, leading in some cases to the opposite result in the orbital interactions. This effect, in turn, partially yields the products not expected on the basis of the starting structure, thus giving rise to the *leakage* phenomenon (the partial loss of *memory effect*).

Experimental Section

Methods

The Potential Energy Surface (PES) was first explored optimizing geometries within the Density Functional Theory (DFT),[15] making use of the composite functionals B3LYP,[16] mPW1PW91[17], and BB1K.[18] Several functionals have already been tested[19] so we choose B3LYP being the most used even in recent papers[20] and mPW1PW91[19c-e,21] and BB1K[12a,19b] being suggested in the more recent papers. From the inspection Tables 2 and 3 we can observe a substantial agreement between the three functionals that show the same qualitative mechanistic picture. The basis set used was Pople's 6-31G(d).[22] Solvent effects were introduced in geometry optimization by the

Polarized Continuum Metohod (PCM)[23] within the universal Solvation Model Density (SMD).[24] All minima and transition structures where fully characterized by vibrational analysis[25] and the zero point energies combined with electronic energies and reported in Tables 2 and 3. The nature of the transition structures (TS) was confirmed by Intrinsic Reaction Coordinate (IRC) optimizations.[26]

The dynamic study was performed within the Born-Oppenheimer Molecular Dynamics model.[27] Energy and gradient were calculated with the HF method[28] and the 3-21G basis set.[29] This level of theory satisfactorily reproduced the DFT surface (see Table 3 and compare Figures 1 and 2 in the Supporting Information) and allowed the calculation of an adequate number of trajectories. We calculated a total of 500 trajectories (250 from TS **II**$_s$ and 250 from TS **II**$_a$).

All calculations were performed using Gaussian 09 software.[30] Figures 1 and 3 and Figures 1 and 2 in the Supporting Information have been obtained by the program Molden.[31]

Acknowledgment. Local funding from the Torino University is gratefully acknowledged.

Supporting Information Available: Cartesian coordinates of all structures, their absolute energies in hartrees and energy difference in kcal/mol and energy profiles for the IRCs are given. This information is available free of charge via the Internet at http://pubs.acs.org.

REFERENCES

(1) Berson, J. A. *Angew. Chem. Int. Ed.* **1968**, *7*, 779–791.

(2) Smith, M. J. ; March, J. in Advanced Organic Chemistry (Eds.: John Wiley & Sons), Hoboken, New Jersey, 2007, Chap. 10, pp. 446–468. ISBN 0-471-72091-7.

(3) Silver, M. *J. Am. Chem. Soc.* **1961**, *91*, 5550–5566.

(4) (a) Berson, J. A.; Reynolds-Warnhoff, P. *J. Am. Chem. Soc.* **1962**, *84*, 682–684. (b) Berson, J. A.; Willner, D. *J. Am. Chem. Soc.* **1962**, *84*, 675–676.

(5) (a) Berson, J. A.; Gayewski, J. J. *J. Am. Chem. Soc.* **1964**, *86*, 5020–5021. (b) Berson, J. A.; Reynolds-Warnhoff, P. *J. Am. Chem. Soc.* **1964**, *86*, 595–609. (c) Berson, J. A.; Willner, D. *J. Am. Chem. Soc.* **1964**, *86*, 609–616. (d) Berson, J. A.; Gayewski, J. J.; Donald, D. S. *J. Am. Chem. Soc.* **1969**, *91*, 5550–5566. (e) Berson, J. A.; Poonian, M. S.; Libbey, W. J. *J. Am. Chem. Soc.* **1969**, *91*, 5567–5579. (f) Berson, J. A.; Donald, D. S.; Libbey, W. J. *J. Am. Chem. Soc.* **1969**, *91*, 5580–5593. (g) Berson, J. A.; Wege, D. ; Clarke, G. M.; Gergman, R. G. *J. Am. Chem. Soc.* **1969**, *91*, 5594–5600. (h) Berson, J. A.; Luibrand, R. T.; Kundu, N. G.; Morris, D. G. *J. Am. Chem. Soc.* **1971**, *93*, 3075–3077.

(6) (a) Collins, C. J. *Acc. Chem. Res.* **1971**, *4*, 315–322. (b) Collins, C. J.; Glover, I. T.; Eckart, M. D.; Raeen, V. F.; Benjamin, B. M.; Benjaminov, B. S. *J. Am. Chem. Soc.* **1972**, *94*, 899–908. (c) Collins, C. J. *Chem. Soc. Rev.* **1975**, *4*, 251–262.

(7) Smith, M. J. ; March, J. in Advanced Organic Chemistry (Eds.: John Wiley & Sons), Hoboken, New Jersey, 2007, Chap. 18, pp. 1570–1572. ISBN 0-471-72091-7.

(8) (a) Goering, H. L.; Sloan, M. F. *J. Am. Chem. Soc.* **1961**, *83*, 1992–1999. (b) Goering, H. L.; Greiner, R. W.; Sloan, M. F. *J. Am. Chem. Soc.* **1961**, *83*, 1391–1397. (c) Goering, H. L.; Towns, D. L. *J. Am. Chem. Soc.* **1963**, *85*, 2295–2298.

(9) (a) LeBel, N. A.; Huber, J. E. *J. Am. Chem. Soc.* **1963**, *85*, 3193–3199. (b) Fraser, R. R.; O'Farrell, S. *Tetrahedron Letters* **1962**, *3*, 1143–1146.

(10) Tests performed with other leaving groups (bromide and nosylate) shown very high and unrealistic barrier possibly due to the lack of explicit solvent molecules.

(11) (a) Tantillo, J. D. *J. Phys. Org. Chem.* **2008**, *21*, 561–570. (b) Williams, A. *Concerted Organic and Bio-Organic Mechanisms*, CRC Press, 2000. (c) Dewar, M. J. S. *J. Am. Chem. Soc.* **1984**, *106*, 209–219. (d) Hess, B. A.; Smentek, L. *Org. Biomol. Chem.* **2012**, *10*, 7503–7509. (e) Tantillo, J. D. *Nat. Prod. Rep.* **2011**, *28*, 1035–1053.

(12) (a) Siebert, M. R.; Zhang, J.; Addepalli, S. V.; Tantillo, D. J.; Hase, W. L. *J. Am. Chem. Soc.* **2011**, *133*, 8335–8343. (b) Siebert, M. R.; Manikandan, P.; Sun, R.; Tantillo, D. J.; Hase, W. L. *J. Chem. Theor. Comput.* **2012**, *8*, 1212–1222. (c) Rehbein, J.; Carpenter, B. K. *Phys. Chem. Chem. Phys.* **2011**, *13*, 20906–20922.

(13) Black, K.; Liu, P.; Xu, L.; Doubleday, C.; Houk, K. N. *PNAS.* **2012**, *109*, 12860–12865.

(14) Ammal, S. C.; Yamataka, H.; Aida, M.; Dupuis, M. *Science* **2003**, *299*, 1555–1557.

(15) (a) R. G. Parr, W. Yang *Density Functional Theory of Atoms and Molecules*, Oxford University Press: New York, **1989**. ISBN 0-19-509276-7. (b) W. Jensen *Introduction to Computational Chemistry*, Wiley; Chichester, **1999**, Chap. 6 ISBN 0-471-98425-6.
(16) (a) A. D. Becke, *J. Chem. Phys.* **1993**, *98*, 5648–5652. (b) W. Koch, M. C. Holthausen *A Chemist's Guide to Density Functional Theory*, Wiley; Weinheim, **2000**, Chap. 6. ISBN 3-527-29918-1. (c) A. D. Becke *Phys. Rev. A* **1988**, *38*, 3098–3100. (d) C. Lee, W. Yang, R. G. Parr *Phys. Rev. B* **1988**, *37*, 785–789.
(17) (a) Adamo, C.; Barone, V. *J. Chem. Phys.* **1998**, *108*, 664–675. (b) Perdew, J. P. in *Electronic Structure of Solids '91*, ed. P. Ziesche and H. Eschrig, Akademie Verlag, Berlin, 1991, p. 11–20.
(18) Zhao, Y.; Lynch, B. J.; Truhlar, D. G. *J. Phys. Chem. A* **2004**, *108*, 2715–2719.
(19) See for example (a) Mackie, I. D.; Govindhakannan, J.; DiLabio, G. A. *J. Phys. Chem. A* **2008**, *112*, 4004–4010. (b) Weitman M.; Major, D. T. *J. Am. Chem. Soc.* **2010**, *132*, 6349–6360. (c) Matsuda, S. P. T; Wilson, W. K.; Xiong, Q. *Org. Biomol. Chem.* **2006**, *4*, 530–543. (d) Hong, Y. J.; Tantillo, D. J. *Org. Biomol. Chem.* **2010**, *8*, 4589–4600. (e) Hong, Y. J.; Tantillo, D. J. *Nat. Chem.* **2009**, *1*, 384–389. (f) Barquera-Lozada, J. E.; Cuevas, G. *J. Org. Chem.* **2009**, *74*, 874–883.
(20) (a) Nguyen, Q. N. N.; Tantillo, D. J. *Beilstein J. Org. Chem.* **2013,** *9*, 323–331. (b) Tantillo, D. J.; von Raguè Schleyer, P. *Org. Lett.* **2013**, *15*, 1725–1727.
(21) (a) Smentek, L.; Hess Jr, B. A. *J. Am. Chem. Soc.* **2010**, *132*, 17111–17117. (b) Hong, Y. J.; Tantillo, D. J. *Chem. Sci.* **2010**, *1*, 609–614.
(22) (a) W. J. Hehre, R. Ditchfield, J. A. Pople *J. Chem. Phys.* **1972**, *56*, 2257–2261. (b) P. C. Hariharan, J. A. Pople Theor. *Chim. Acta* **1973**, *28*, 213–222. (c) T. Clark, J. Chandrasekhar, P. v. R. Schleyer *J. Comput. Chem.* **1983**, *4*, 294–301. (d) M. J. Frisch, J. A. Pople, J. S. Binkley *J. Chem. Phys.* **1984**, *80*, 3265–3269.
(23) (a) Barone, V.; Cossi, M. *J. Phys. Chem. A* **1998**, *102*, 1995–2001. (b) Cossi, M.; Rega, N.; Scalmani, G.; Barone, V. *J. Chem. Phys.* **2001**, *114*, 5691–5701. (c) Cancès, M. T.; Mennucci, B.; Tomasi, J. *J. Chem. Phys.* **1997**, *107*, 3032–3041. (d) Cossi, M.; Barone, V.; Mennucci, B.; Tomasi, J. *Chem. Phys. Lett.* **1998**, *286*, 253–260. (e) Mennucci, B.; Tomasi, J. *J. Chem. Phys.* **1997**, *106*, 5151–5158.
(24) (a) Marenich, A. V.; Cramer, C. J.; Truhlar, D. G. *J. Phys. Chem. B* **2009**, *113*, 6378–6396. (b) Marenich, A. V.; Cramer, C. J.; Truhlar, D. G. *J. Phys. Chem. B* **2009**, *113*, 4538–4543.
(25) Reaction enthalpies and free energies were computed as outlined, for instance, in: Foresman,J. B.; Frisch, Æ. *Exploring Chemistry with Electronic Structure Methods*, Gaussian, Inc., Pittsburgh, PA (USA), **1996**, pages 166–168.
(26) Gonzalez, C.; Schlegel, H. B. *J. Chem. Phys.* **1989**, *90*, 2154–2161. Gonzalez, C.; Schlegel, H. B. *J. Phys. Chem.* **1990**, *94*, 5523–5527, and references therein.
(27) (a) T. Helgaker, E. Uggerud, H. J. A. Jensen *Chem. Phys. Lett.* **1990**, *173*, 145–

150. (b) E. Uggerud, T. Helgaker *J. Am. Chem. Soc.* **1992**, *114*, 4265–4268. (c) W. Chen, W. L. Hase, H. B. Schlegel *Chem. Phys. Lett.* **1994**, *228*, 436–442. (d) J. M. Millam, V. Bakken, W. Chen, W. L. Hase, H. B. Schlegel *J. Chem. Phys.* **1999**, *111*, 3800–3805. (e) X. Li, J. M. Millam, H. B. Schlegel *J. Chem. Phys.* **2000**, *113*, 10062–10067.

(28) (a) C. C. J. Roothan, *Rev. Mod. Phys.* **1951**, *23*, 69–76. (b) J. A. Pople, R. K. Nesbet, *J. Chem. Phys.* **1954**, *22*, 571–572. (c) A. Szabo, N. S. Ostlund *Modern Quantum Chemistry*, McGraw-Hill; New York, **1982**, Chap. 3. ISBN 0-07-062739-8.

(29) J. S. Binkley, J. A. Pople, W. J. Hehre, *J. Am. Chem. Soc.* **1980**, *102*, 939–947.

(30) Gaussian 09, Revision A.1, Frisch, M. J.; Trucks, G. W.; Schlegel, H. B.; Scuseria, G. E.; Robb, M. A.; Cheeseman, J. R.; Scalmani, G.; Barone, V.; Mennucci, B.; Petersson, G. A.; Nakatsuji, H.; Caricato, M.; Li, X.; Hratchian, H. P.; Izmaylov, A. F.; Bloino, J.; Zheng, G.; Sonnenberg, J. L.; Hada, M.; Ehara, M.; Toyota, K.; Fukuda, R.; Hasegawa, J.; Ishida, M.; Nakajima, T.; Honda, Y.; Kitao, O.; Nakai, H.; Vreven, T.; Montgomery, Jr., J. A.; Peralta, J. E.; Ogliaro, F.; Bearpark, M.; Heyd, J. J.; Brothers, E.; Kudin, K. N.; Staroverov, V. N.; Kobayashi, R.; Normand, J.; Raghavachari, K.; Rendell, A.; Burant, J. C.; Iyengar, S. S.; Tomasi, J.; Cossi, M.; Rega, N.; Millam, N. J.; Klene, M.; Knox, J. E.; Cross, J. B.; Bakken, V.; Adamo, C.; Jaramillo, J.; Gomperts, R.; Stratmann, R. E.; Yazyev, O.; Austin, A. J.; Cammi, R.; Pomelli, C.; Ochterski, J. W.; Martin, R. L.; Morokuma, K.; Zakrzewski, V. G.; Voth, G. A.; Salvador, P.; Dannenberg, J. J.; Dapprich, S.; Daniels, A. D.; Farkas, Ö.; Foresman, J. B.; Ortiz, J. V.; Cioslowski, J.; Fox, D. J. Gaussian, Inc., Wallingford CT, 2009.

(31) Schaftenaar, G.; Noordik, J.H. "Molden: a pre- and post-processing program for molecular and electronic structures" *J. Comput.-Aided Mol. Design* **2000**, *14*, 123–134.

Table of Content Graphic